

## Analysis of Existing Designs for FPGA-Based Ultrasound Imaging Systems

Keenan Chatar<sup>1</sup> and Marcus Lloyd George<sup>2</sup>

<sup>1</sup>*Electrical and Computer Engineering*

*University of the West Indies, San Juan, Trinidad and Tobago*

<sup>2</sup>*Dept. Electrical and Computer Engineering*

*University of the West Indies St. Augustine, Trinidad and Tobago*

<sup>1</sup>*keenan.chatar@my.uwi.edu*, <sup>2</sup>*Marcus.George@sta.uwi.edu*

### Abstract

*The purpose of this paper is to compare, analyse and summarize the designs of existing emergency medical service ultrasound machines and evaluate the results obtained from each design to determine the most efficient and effective system. The medical ultrasound has been developed based off sonar technology and enables users to visualize the internal tissue structure of various biological organisms in real time. With the evolution and advances of analog technologies, digital processing and manufacturing, ultrasound systems can spread to different applications. In addition to this, as these technologies shrink in size and cost, they become more available to healthcare applications. Various designs for ultrasound systems are available, however the most efficient and effective design is not known. This paper seeks to compare and contrast three design choices and their produced results made in current literature and the produced results from the designs of portable ultrasound systems.*

**Keywords:** *component; Field Programmable Gate Array; Ultrasonography; Ultrasonic Imaging; Medical imaging; Ultrasound system; FPG*

### 1. Introduction

Ultrasound machines operate by transmitting focused beams of sound wave energy into the body. Using the differences in strength and the delay of the reflected sound wave, images of the biological tissue can be reconstructed onto a display [1]. This is usually accomplished with a piezoelectric-based transducer array situated at the end of a probe module, which is pressed against the body being imaged. The piezoelectric transducer elements are stimulated by high-voltage (5 VPP–300 VPP) pulses, causing them to vibrate, which in turn generates the transmitted acoustic waves. The elements in the array are phase aligned with each other to create a focused beam of acoustic waves at a predetermined location and distance in the body. As these incident waves pass through the subject, the acoustic impedance differences between layers of tissue cause reflections back to the transducer. Immediately after transmitting acoustic waves, the transducer elements become detectors, picking up the reflected signals. A representative image of the body is formed by focusing the transmit beam along hundreds of scan lines in the area being analysed, and then reassembles them in the backend electronics to form a 2-D image. 3-D ultrasounds are possible by mechanically moving the transducer array or electronically steering the beam direction along a secondary axis. Ultrasonic technology is utilized in a wide variety of fields for uses such as object detection, measuring distances and numerous medical applications. In medicine, ultrasonography is a simple, dynamic imaging module which is used for visualization of body structures and various internal organs [2]. In most modern ultrasound imaging systems, it usually consists of an

ultrasound transmit and receive module called the beamformer which comprises of the digital Transmitter (Tx) and Receiver (Rx) beamformer. The transmit module is responsible for generating the necessary logic pulses with the required timing and phase to cause electronic steer and focus of the acoustic beam to form 3-D images. The receive beamformer is responsible for receiving the echo from the acoustic wave from the tissue at the analog front end. This data is then sampled, collated and analysed to form the representative information in the B-mode image. However, these modules usually have a style of architecture that limits the access to the ultrasound module thus restricting the modifications and improvements to suit the application. [2]. To achieve miniaturization and cost reduction as well as longer battery life, these portable ultrasound machines take advantage of the continuing advances in solid-state technologies, such as application-specific integrated circuits (ASICs) [3]. However, the ASIC approach is usually tailored toward a specific method or application and thus limits its usefulness. Thus, to improve the usability and overall application, FPGAs can be used to improve the ability for ultrasound imaging systems to create small form factor and high-performance products with reduced power consumption [4]. The use of FPGAs in the system designs include an improved functional flexibility for the various imaging systems to adapt quickly to the continuously evolving clinical applications. In addition to this, the programmable approach to diagnostic imaging systems, especially in the field of computational capabilities, were evaluated in [5-6]. In modern times, various portable ultrasound machines have been developed for various applications, such as ambulatory and medicine, intensive care *e.g.* [5-8]. The purpose of this paper is to compare the designs of some existing ultrasound machines and evaluate the results obtained from each design to determine the most efficient and effective design.

## 2. First Design

For the first system created by [3], we can see in Figure 1 below which illustrates the overall system block diagram of the developed system. The entire system was developed as a low-cost portable system which is configured on one single FPGA chip. The diagram illustrates the scanner modules, the FPGA module, the power supply/ battery and the control module. The scanner module is a 16 wide channel that comprises of the analog front end which in turn houses components such as analog to digital converters, analog receivers, transmit pulsers and its associated pulse drivers. The system components are specified in Table 1.

**Table 1. System Specification [3]**

<b>Analog Front End</b>	
Drivers	Eight pulser drivers
Pulsers	16 high-voltage (HV) pulser
MUXs	eight HV multiplexers (MUXs)
ADCs	2 eight-channel 12-bit ADC chips

The FPGA chip is used for supporting the receive beamformer (Rx) and also for processing the mid, backend and also B-mode image enhancements. In additions, it also supports the transmit beamformer (Tx) is generating transmit pulse patterns . The FPGA also handles the real time controlling of the system by interfacing with a Samsung S3C6410 mobile processor to handle the sub-system control, image display and communication

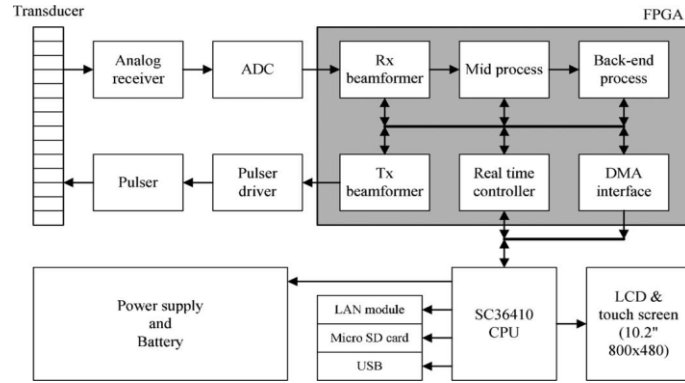


**Figure 1. Overall System Block Diagram [3]**

**A. Front End**

In medical ultrasound imaging, the receive beamforming is used for improving spatial and contrast resolution. As shown in Figure 2, the receive beamforming can be represented by  $rbf(n)$ .

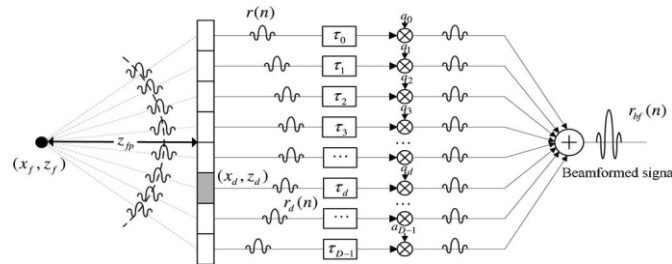


**Figure 2. Receive Beamforming Representation**

In this illustration, the ultrasonic signal falls onto the physical channel D in the receive beamforming method, which then forms the  $r_d$  receive signal based on an apodization coefficient and receive focusing delay. These receive signals are then summed to form the beamformed signal. This signal is then sampled by the ADC to be sent for processing in the Mid-Back End module. In dynamic receive beamforming used in this design, as shown in Figure 3 (a) below, we can see that the focusing delay is updated at each beamforming point, at each respective channel, thus this an lead to an increase in the complexity of the hardware used. A solution was employed to reduce this potential high complexity. This was done by updating the focusing delay at specific zones as opposed to every beamforming focal point, thus reducing the necessary hardware complexity. This process is illustrated in Figure 3(b).

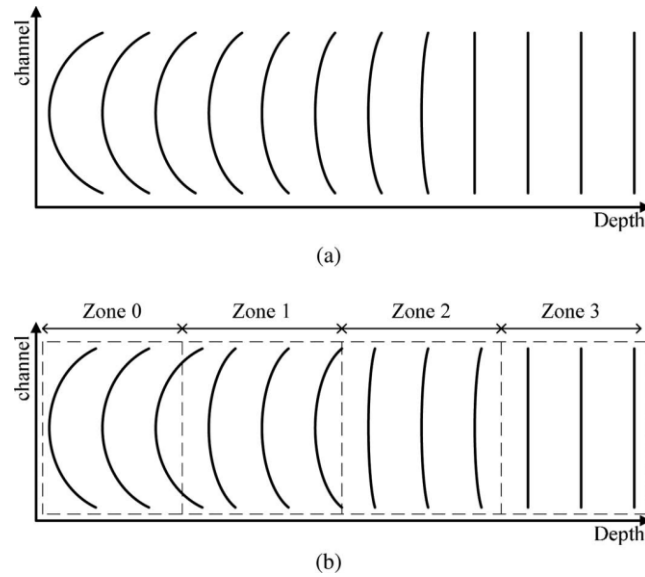


**Figure 3. Illustrates the Focusing Delay Update Patterns for (a) Conventional Focusing (b) Pseudo-dynamic Focusing.[3]**

*B. Mid and Back End*

The Figure 3. below illustrates the block diagram and all of the functional modules within the respective mid and back end processes.

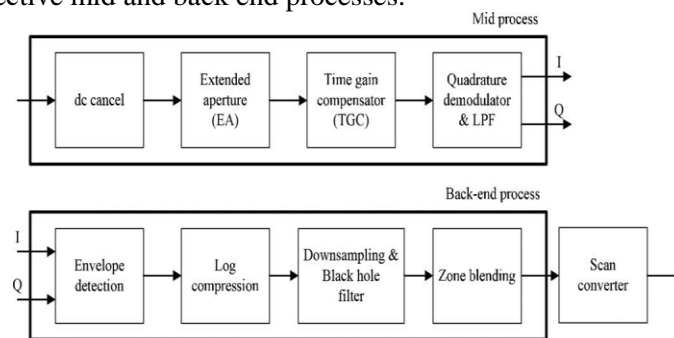


**Figure 4. Functional Block Diagram [3]**

1) *Mid Processing*: As we can see from the figure above, DC cancelling is first applied to the post beamformed signal to remove the undesired DC component from the ADC. Next the Extended Aperture block receives two receive ultrasound data points sequentially. In addition, the Time Gain Compensator (TGC) is applied to the signal to generate a well balanced ultrasound image. To obtain the necessary baseband data, quadrature demodulation is applied. In addition, further processing at the back end is required.

2) *Back End Processing*: To obtain the envelope of data from the obtained ultrasound signal, the method of envelope detection is applied to the information passed from the mid processing to obtain the complex baseband data. In addition, the log compression is applied to reduce the dynamic range of the data. Furthermore, a black hole filter and zone blending modules are incorporated and applied for image enhancement. The final scan module then converts the data which is in polar coordinates to a Cartesian coordinate system, to then be plotted onto the data display.

### 3. Second Design

Figure 5 below illustrates the overall system block diagram for the portable ultrasound machine developed by [9] and its functional modules. The system comprises of a scanner module and a power module. The ultrasound scanner module comprises of various analog front end components [beamformer receiver (Rx) and transmitter (Tx), transducers, ADCs, pre-amplifier, variable gain amplifier] and also digital mid and back end components [Timing controllers, digital I/O interface].

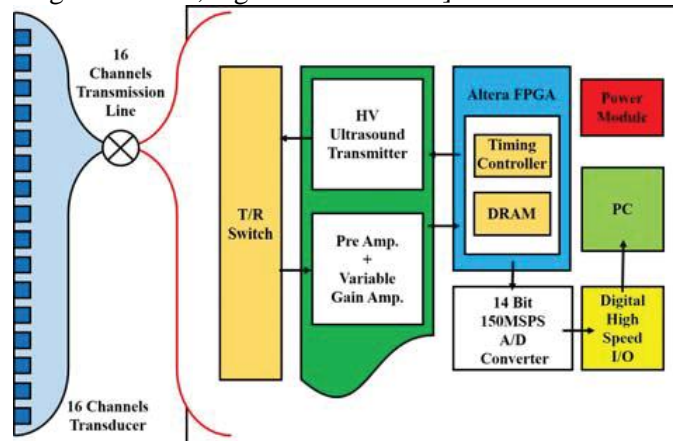
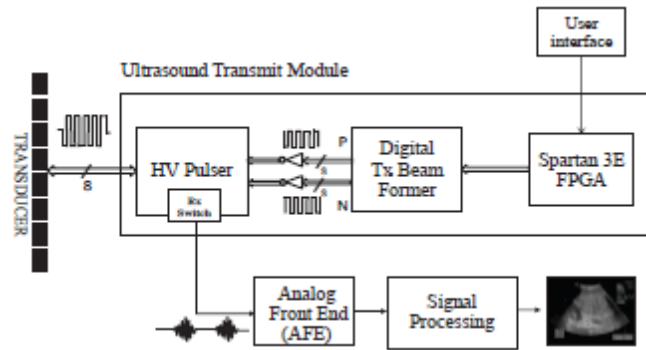


Figure 5. Overall Block Diagram [9]

The timing controller found in the FPGA module controller provided timing control for the High Voltage (HV) ultrasound transmitter (Tx) which enabled its pulse repetition frequency (PRF). The transmitter allowed the PRF to produce a pulse and simultaneously excite the transducers for the ultrasonic pulse via a designed protection circuit. After this pulse was transmitted, the subsequent echo signals were then received via a limiter which then passed the signal through a pre-amplifier and variable gain amplifier to amplify the received signal with a gain of approximately 50dB. This amplified signal was then sampled by the 150MSPS 14-bit resolution ADC module to digitize the analog signal to be fed to the FPGA board. After receiving the digital signal, the FPGA sends the data to the computer via the high speed digital I/O which operates at a maximum 50MHz clock rate. The FPGA board was used as the main controller for the system. The board contained two important modules which were the timing controller used for the PRF and the imaging processor. As explained before, the FPGA timing controller provided the necessary timing for producing the ultrasonic pulses via the PRF. The transducers that are used by the system are curved, and thus the information obtained will be in polar coordinates, thus before the final plot of the data is made, it is transformed to Cartesian coordinates via a linear interpolation algorithm in the FPGA.

### 4. Third Design

The diagram in Figure 6 below illustrates the ultrasound imaging system architecture created by [10]. The system comprises of a High Voltage (HV) Pulser which generates the ultrasonic acoustic waves in the target area of interest. It also comprises of a digital beamformer transmitter (Tx), the FPGA board which houses the digital modules, the user interface which comprises a display screen, the Analog front end components, and also the signal processing module.



**Figure 6. Imaging System Architecture [10]**

### A. Transducer Array

The transducer array used for this system has two main modes of excitation: 1) Phased and 2) Linear. In the Phased Array mode, the elements of the transducer are excited to focus the acoustic waves onto a single focal point. However, in the Linear Array mode, only a subset of the transducer elements are excited. The phased array mode is depicted in Figure 7. The phased and linear modes are used in concert to scan the organ of interest as the excitation of the elements would form multiple focal points of ultrasound beams which can then generate the required echo information.

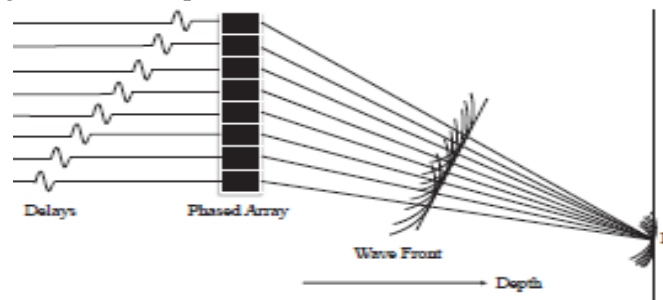


**Figure 7. Operation of Phased Array Mode. [10]**

### B. FPGA Based Acoustic Beam Steering

The direction, and depth of focus of the acoustic beam is controlled by the FPGA Spartan 3E. This ability to steer and focus the beam allows the generation of 3D-images. To generate this acoustic beam steering, the FPGA calculates and delays each transducer element excitation by a certain amount of time to generate the required beam direction, focus and angle. The FPGA is also tasked with generating a control signal to manage the pulse repetition rate which would be based on the depth of interest [7].

### C. Digital Tx Beamformer

To transmit and also enable acoustic beam steering, a programmable digital transmit module is developed within the FPGA. This module is capable of generating phased logic pulses to be sent to the transducer elements which in turn would delay the logic pulses by the elements to focus the ultrasound beam. This control of the beam will also enhance the received image and improve resolution. The beamformer can be programmed via programmable registers.

#### D. HV Pulser

The High Voltage (HV) pulser acts simply to amplify the digital outputs of the beamformer. The HV pulser also acts as a switch based on the two logical inputs. If the inputs are high, then the circuit can act as a switch to receive low voltage signals of the reflected ultrasound waves, this also reduces the load on the front end receive circuitry. If the inputs are logic low, the outputs of the pulser would then be low. Finally, if the inputs are different logic, then the system will generate high voltage signals as normal.

#### E. User Interface

A simple graphical user interface was developed using Microsoft Windows as a platform. The GUI was created using National Instruments LabVIEW program. This FPGA Spartan-3E can interface with the GUI via a USB connection to the PC. This user interface would allow the variation of transmission parameters and modifications during measurements when necessary.

### 5. Experimental Results

#### A. First Design

Figure 8 illustrates a prototype of the developed system by [3]. The required system specifications and the parts that are used for the construction of the system is found in Table II below.

**Table 2. System Specification [3]**

System Specification	Parts Used
Mode	B-mode, BM-mode
Size	245mm x 190mm
Weight	560g
Power	External/Battery
Probe	3.5MHz convex and 7.5 MHz Liner array
Display	10.2 inch TFT LCD (800x480)
CPU	Samsung S3C6410 at 667MHz
OS	Linux kernel 2.6.21
System Memory	256MB (SDRAM), 4Gb (Flash)
FPGA	Xilinx Spartan-3 (XC3S4000)
Peripherals	USB, Micro SD, LAN, DVI
Display Mode	Dual and Quad B-mode
Cine	256 frames

As we can see in Figure 8. (a), this illustrates a sample of the captured image from the 3.5MHz convex array transducer. Figure 8.(b) illustrates the capture image from the 7.5Mhz linear array transducer setup. The images captured were of two phantom materials that mimic the parameters of tissue at a depth of 14 and 4 cm. Based on the outputs, we can clearly see the target material up to a depth of approximately 13 cm. In addition, the linear array also showed clear visuals up to the 4 cm depth.

The modules that were developed and embedded for the FPGA chip used a total of 46, 41, 93 and 86% of slide flip flops block RAMs, 4-input LUTs and multipliers [3]. This

indicates that all the modules of the system can be managed by the fairly inexpensive Spartan-3 FPGA chip. The system implemented the use of a battery power module which provided and estimated 1.5 hour battery life in a high intensive continuous scan.

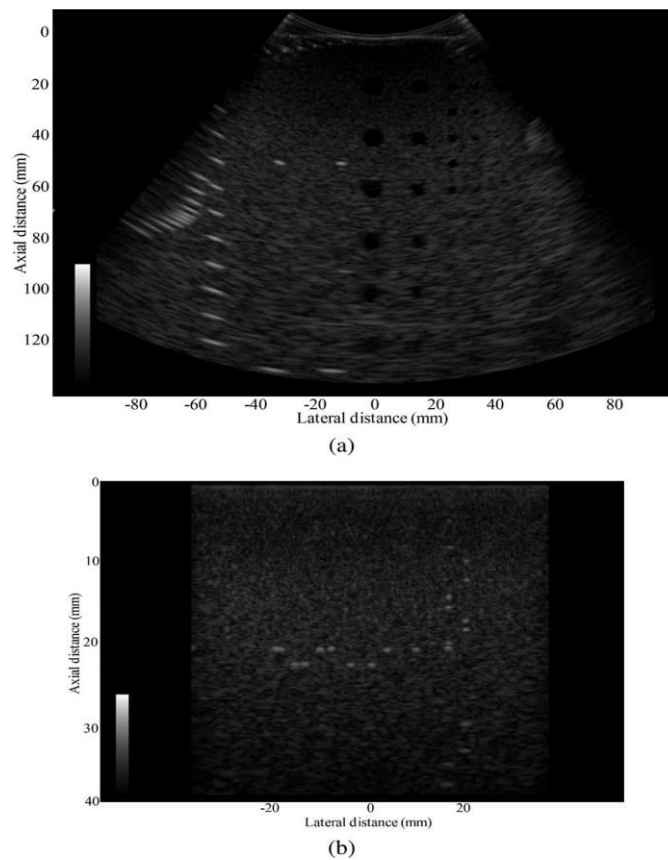


**Figure 8. Ultrasound Images of Phantoms by Design 1 a) Convex 3.5MHz Probe. b) Linear 7.5MHz Probe. [3]**

### *B.Second Design*

For the design developed by [9], the completed prototype is illustrated in Figure 9 below. The main developed hardware systems comprises of the following main hardware modules: 1) Txbeamformer, 2) High Voltage Pulser 3) AFE Module and the FPGA module. This setup is connected to a PC, which runs a custom software containing a custom user interface.



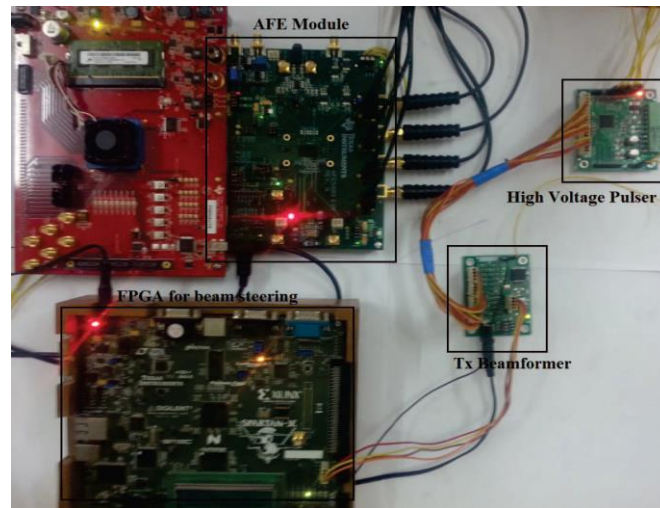


**Figure 9. Completed Prototype [9]**

.An experiment was conducted which was designed to transmit various ultrasound pulses into a phantom material which mimicked human tissue to acquire and display the B-mode image. The FPGA module is utilized to employ the necessary beam steering to obtain a better image. The reflected echo signals are received, filtered and digitized by the AFE module. A Delay and Sum algorithm is implemented to receive the echoes based on different depths, compensate this discrepancy in phase, and then calculate the information to generate a summed receive beam to be accepted into the FPGA. This output data is then accepted by the FPGA to be de-serialized, and signal processing algorithms are applied to construct the B-mode image. The types of signal processing applied to construct the B-mode image includes log compression, envelope detection and scan conversion. We can see in Figure 10. the constructed image and the ultrasound system developed by [9].

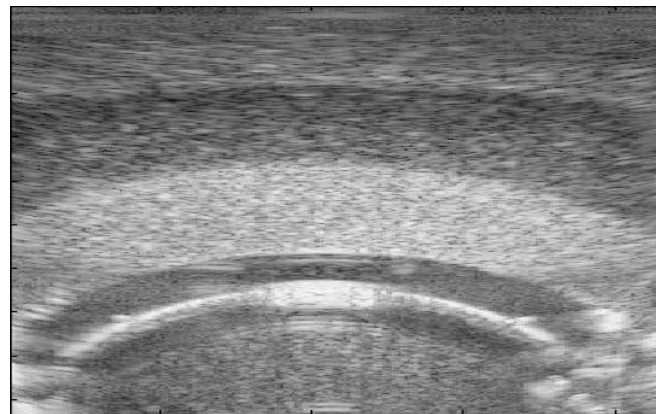


**Figure 10. Ultrasound Image of Phantom for Design 2 [9]**

### C.Third Design

The developed system by [10] is illustrated in Figure 11. below. The main system components includes a custom 16 channel transducer that was specifically developed for this application, an ADC, digital interface and an Altera FPGA board.

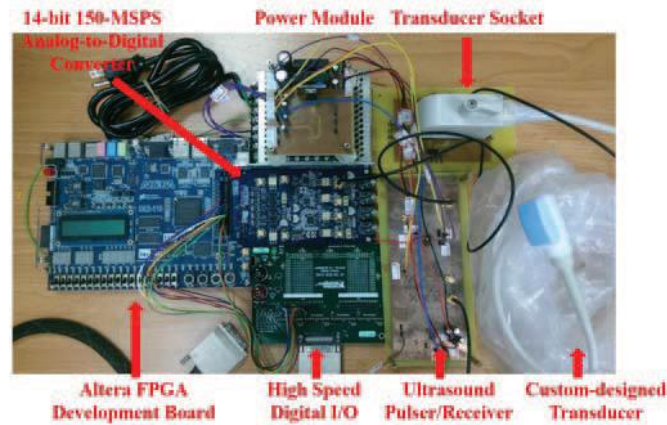


**Figure 11. Developed Prototype System for Design 3 [10]**

The main features of the developed system is summarized below:

- A total of 8 independent channels used to transmit and drive the transducer elements. This can be further extended to house 8 more channels.
- A serial interface designed for a data rate of up to 80Mbps.
- User interface and display which allows users to select or modify various parameters.
- Produces a maximum ultrasound output bandwidth of 80MHz.
- Low hardware complexity and an approximate cost of \$166.
- Maximum ultrasound transmit output bandwidth 80 MHz.

The transducer was covered with gel and placed on the skin of the neck. Therefore, it can be clearly display the contour of tongue base. The participant was first instructed to remain still and silent during the measurements and to breathe normally and avoid tongue movement, swallowing or talking. An illustration of the results obtained is shown in Figure 12.

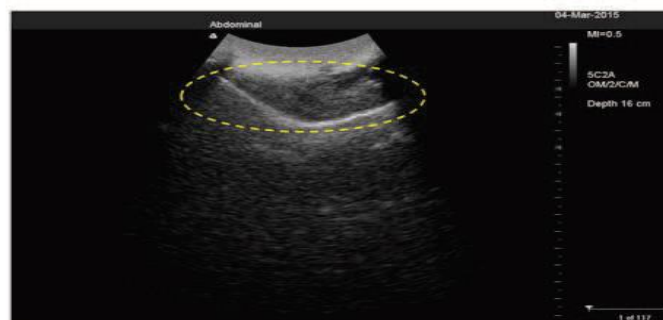


**Figure 12. Ultrasound Image Result [10]**

## 6. Comparison of Results

In comparison, we can see that for the first design, a large emphasis was placed on the development of the Analog Front End circuitry as the entire front end was manually calculated and designed independently for the specific application. The 16 channel transducer used provided more receive signals as opposed to the 8-channel method in

design 3. This increase in channels increased the accuracy for the data sampling at the ADC, however this in turn also increased the hardware complexity and cost. Design 2 also had a lower complex hardware requirement however the cost of the design was significantly larger than design one as design one succeeded in using a single cost effective FPGA chip to house the necessary computational module requirements. Design One developed a method of implementing a focusing delay for the system while reducing the hardware complexity. This method had little reduction in system quality and output. In addition to this, for design one, a separate processor is used for the controller action by means of the Samsung S3C6410 processor.

For designs 1 and 2, the same type of gelatin phantom is used to test and evaluate the results of the systems. Design 2 is capable of B-mode imaging, however design 1 also allowed for BM-mode imaging. The design 1 also allowed for multiple image displays (up to 4) while the design 2 only allowed for 2 while design three only allowed one image output. In comparison of the produced sample outputs, it is clear that the first design produces a more accurate, defined and clear output in comparison to design 1 or 2. 7.

## 7. Conclusion

In this paper, three different designs for portable ultrasound imaging systems were analyzed and compared. The results for each design was also documented and compared to determine the most efficient and overall outstanding product. Each product analyzed employed different design paths, in which each had their own different results. Various criteria were considered in comparing the results including but not limited to: Cost, Imaging Quality, Power Consumption, Size, Weight *etc.* Further investigations and analysis can be carried out to elicit information such as the best quality producing designs to develop a prototype based on aggregated design specifications.

## References

- [1] V. Chan and A. Perlas, "Basics of Ultrasound Imaging", S.N. Narouze (ed.), Atlas of Ultrasound-Guided Procedures in Interventional Pain Management, DOI 10.1007/978-1-4419-1681-5 2, Springer Science+Business Media, LLC, (2011).
- [2] M. Tsakalakis and N. Bourbakis, "A Wearable Ultrasound Multi-Transducer Array System for Abdominal Organs Monitoring." Paper presented at the Bioinformatics and Bioengineering (BIBE), 2013 IEEE 13th International Conference on, (2013), November 10-13.
- [3] G. D. Kim, C. Yoon, S. B. Kye, Y. Lee, J. Kang, Y. Yoo and T. K. Song, "A single FPGA-based portable ultrasound imaging system for point-of-care applications", Ultrasonics, Ferroelectrics, and Frequency Control, IEEE Transactions on, vol. 59, no. 7, (2012), pp. 1386-1394.
- [4] J. Alexander, "Xilinx Devices in Portable Ultrasound Systems", WP378, vol. 2, (2013) May 13.
- [5] A. Agarwal, F. K. Schneider, Y. M. Yoo and Y. Kim, "Image quality evaluation with a new phase rotation beamformer," IEEE Trans. Ultrason. Ferroelectr. Freq. Control, vol. 55, no. 9, (2008), pp. 1947-1955.
- [6] F. K. Schneider, Y. M. Yoo, A. Agarwal, L. M. Koh and Y. Kim, "New demodulation filter in digital phase rotation beamforming," Ultrasonics, vol. 44, no. 3, (2006), pp. 265-271.
- [7] C. Basoglu, R. Managuli, G. York and Y. Kim, "Computing requirements of modern medical diagnostic ultrasound machines" Parallel Computing, vol. 24, (1998) September.
- [8] B. G. Tomov and J. A. Jensen, "A new architecture for a single-chip multi-channel beamformer based in a standard FPGA," in Proc. IEEE Ultrasonics Symp., (2001), pp. 1529-1533.
- [9] C. K. Weng, J. W. Chen and C. C. Huang, "A FPGA-based wearable ultrasound device for monitoring obstructive sleep apnea syndrome." In Ultrasonics Symposium (IUS), 2015 IEEE International, IEEE, (2015), pp. 1-4.
- [10] C. Dusa, P. Rajalakshmi, S. Puli, U. B. Desai and S. N. Merchant, "Low complex, programmable FPGA based 8-channel ultrasound transmitter for medical imaging researches." In e-Health Networking, Applications and Services (Healthcom), 2014 IEEE 16th International Conference on, IEEE, (2014), pp. 252-256.
- [11] G. D. Kim, Y. Changan, S. B. Kye and Y. Lee, "A Single FPGA Based Portable Ultrasound Imaging System for Point of Care Applications", IEEE Transactions on Ultrasonics Ferroelectrics and Frequency Control, vol. 59, no. 7, (2012), pp. 1386-1394.

